Proceedings of The Twelfth (2002) International Offshore and Polar Engineering Conference
Kitakyushu, Japan, May 26−31, 2002
Copyright © 2002 by The International Society of Offshore and Polar Engineers
ISBN 1-880653-58-3 (Set); ISSN 1098-6189 (Set)

Wave Drift Added Mass Of Floating Bodies Measured From a Free Decay Test Or a Slowly Forced Oscillation Test In Waves

Takeshi Kinoshita, Weiguang Bao, Motoki Yoshida and Kazuko Ishibashi
Institute of Industrial Science, University of Tokyo
Tokyo, Japan

ABSTRACT

When a body is slowly oscillating in waves, there exists another source of added mass and damping, i.e. the so-called wave drift added mass and wave drift damping. They are resulted from the nonlinear interaction between the slow oscillations and the waves. Different from the conventional added mass and wave-radiating damping, they are quadratic forces in wave amplitude. The wave drift added mass is measured in the present work from a free decay test or a forced slow oscillation test. The model is either a circular cylinder or an array of four circular cylinders. Experimental parameters are systematically changed to examine their effects on the wave drift added mass. A calculation based on the potential theory is also carried out. Measured wave drift added mass are presented and compared with the calculated results in the present work.

KEY WORDS: nonlinear wave loads, drift motion, wave drift damping, wave drift added mass.

INTRODUCTION

Ocean structures are usually constrained by mooring systems, which supply relatively weak restoring forces in horizontal plane. Under the slowly varying drift forces exerted by ocean waves, these structures may undergo low-frequency resonant oscillations in the horizontal motion modes, i.e. surge, sway and yaw.

Conventional added mass and damping can be obtained by solving a linear radiation problem in which the body of the structures is forced to oscillate in the calm water. In the case when the frequency of the resonant motion is very small, the wave-radiation damping is negligibly small, while the added mass is the same order of the displaced water mass. However, with the presence of the incident waves, there exists another kind of added mass and damping that is caused by the nonlinear interaction between waves and slow oscillations. As part of the nonlinear wave loads, their magnitude is proportional to the square of the wave amplitude, which is different from the conventional added mass and damping, and they are called wave drift added mass and wave drift damping respectively. Recently many studies [2~7, 10~15] have been made to evaluate and measure the wave drift damping which is much more significant compared with the conventional wave-radiating damping and plays a key role in slow drift motions. On the other hand, wave drift added mass is considered less important and relatively less attention has been paid to it. But it is of the same order in magnitude as the wave drift damping. Since it is important to simulate the time series accurately for designing a dynamic positioning system. It is worthwhile to know more about the wave drift added mass because it might change resonant frequency and affect time series of the slow drift motion of the floating structures. For example, in one typical free decay test of our experiments, it is observed that the resonance frequency is shifted from 0.553 rad/sec to 0.532 rad/sec due to the effects of the wave drift added mass.

In this study, the wave drift added mass is measured by a series of experiments, which consists of two kinds of tests, i.e. a free decay test and a forced slow oscillation test made in waves. The model of the experiments is either a single circular cylinder or an array of circular cylinders. Experiment parameters, such as the draft of the models, wave amplitude and length, the frequency of the forced oscillation, are systematically changed to examine their effects on the wave drift added mass. A method to calculate the wave drift added mass is discussed in the present work as well. The calculation is based on the potential theory. A coordinate system following the slow oscillation is adopted and two time scales are used to describe the wave motions and slow oscillations respectively. It is found that higher order potentials in terms of slow frequency make contributions to the wave drift added mass although it is difficult to solve these potentials. Comparison between the experimental and calculated results is made to verify the present theory.

A description of experiment arrangement and a brief discussion on the analysis method of measured data are presented in the next section. It is followed by a section to discuss the method of calculation. Experimental results are shown and compared with calculated ones in the fourth section and concluding remarks are addressed in the last section.

EXPERIMENT ARRANGEMENT

Experiments to measure the wave drift added mass are carried out in the Ship Maneuvering Research Basin belonging to Tokyo University of Mercantile Marine, which is 54 meters long and 10 meters wide with a depth of 2 meters. According to our previous experience, sufficient data can be measured and recorded in this size of towing tank before the sidewall reflection affects the experiment results.

Experiment Models

A single circular cylinder and an array of four circular cylinders are used as models in the experiments. The radius of cylinder, denoted by a, is equal to 0.125 meter and the draft, designated by d, changes from a to $3a$. When the cylinder array is used, the cylinders are located at the corners of a rectangular, which is L=10a long and B=5a wide. The principle particulars of the models are presented in Table 1 and schematic figures of the cylinder array are shown in Fig 1.

Table 1. Principle particulars of models

Model	Radius a (m)	Distance between cylinders (m)		Draft d (m)	Total weight W (kg)
		Longitude	Transverse		
Single cylinder	0.125	——	——	0.125 0.250	9.190
Cylinder array		1.250	0.625	0.375	62.230

Setting-Up Of Models

As shown in Fig 2, the models are hung up by four wires, which have an average length of about 4.5 meters. The length of the wires is adjusted according to the draft of the models. The weight of the wires is negligible when the natural frequency of the whole system is evaluated.
In order to make a forced oscillation, the models are connected to a carriage through soft springs, the spring constant of which is 0.001~0.0015 kgf/mm in the case of a single cylinder and 0.006 kgf/mm for the cylinder array. The springs are used to absorb linear wave forces. The carriage is driven to move along a pair of rails by a servomotor so that it leads the models to oscillate slowly in surge direction.
The displacement of the models is measured by an optical position sensor system. A pair of cantilever load cells, which connects the soft spring and the carriage, is used to measure the forces acting on the models.

Experiment Conditions

Two kinds of tests are performed, i.e. a free decay test (denoted as FD) and a forced oscillation test (designated as FO). In the FD tests, the models are disconnected from the carriage and the forces acting on the models are not measured. Only the displacement of the models is measured.

Table 2. Range of experimental parameters.

Model		Single cylinder	Cylinder array
Wave amplitude ζ_a (m)		0.020, 0.030, 0.040, 0.050, 0.060	
Wave frequency ω (rad/sec)		3.96~8.85	
Amplitude of forced oscillation $\bar{\xi}$ (m)		0.100	
Frequency of forced oscillation σ (rad/sec)	d=3a	0.641, 0.804, 1.055	0.691
	d=2a	0.772	0.929
	d=a	1.162	1.137, 1.287, 1.444

When FO tests are performed, the models are connected to the carriage through the soft springs and cantilever load cells as mentioned in the previous subsection. Both the displacement and the forces are measured. The frequency of the forced slow oscillation is set to be a little bit higher than the natural frequency of the whole test system.
Approximate forty FD tests and four hundred FO tests are performed in a systematic combination of experimental parameters, i.e., the wave amplitude and frequency, amplitude and frequency of the forced oscillations. Shown in Table 2 is the range of these parameters

Restoring Force Coefficient

The models are hung up by four wires as mentioned previously. The whole experiment system can be treated as a pendulum. Therefore, a restoring force will be generated when the model departs from its equilibrium position. In order to abstract added mass from the measured data accurately, it is necessary to measure this restoring force precisely. This is done by pulling the model from and then back to its equilibrium position, step by step, through a ring-type load cell. At each step, distance x, from the equilibrium position and the restoring force f_r are measured. It is assumed that the restoring force f_r is proportional to the distance x_s in the range of the forced oscillation amplitude, i.e. $f_r = Cx \text{ if } x \le \bar{\xi}$. The measured data are plotted and a straight line is drawn by least square method. The restoring coefficient C is determined from the slope of the straight line. The results are shown in Table 3 for each draft. The measured restoring coefficient will be used in the dynamic analysis later.

Table 3. Restoring coefficient of the model system

Draft d (m)	Single cylinder		Cylinder array	
	Ballast weight W (kg)	Restoring coefficient C (N/m)	Ballast weight W (kg)	Restoring coefficient C (N/m)
0.375	12.0	6.79	20.0	20.91
	15.0	12.85		
	20.0	23.74		
0.250	6.0	7.22	0	30.40
0.125	0	7.50	0	89.29

Analysis Of Experimental Data

The method to analyze FD (free decay) tests is a routine work now. Detail discussion of it will be omitted here. Only the equations to evaluate added mass are given below:

$$M_s = C/\sigma_s^2 - (M_m + M_b) \tag{1a}$$

$$M_w = C/\sigma_w^2 - (M_m + M_b) - M_s \tag{1b}$$

where M_m and M_b are mass of the model and ballast respectively. C is the restoring coefficient mentioned in the previous subsection while σ_s and σ_w denote the frequency of the free decay tests in still water and in waves respectively. In Eqs. 1a and 1b, M_s is the added mass measured in still water tests while M_w is the change of added mass due to waves or the so-called wave drift added mass that we are looking for.
To analyze the measured data of FO (forced oscillation) tests, the method used by Kinoshita et al. [8][9] is adopted. The equation of forced low-frequency oscillations in still water and in waves can be expressed as follows respectively,

$$(M_m + M_b + M_s)\ddot{x} + \tfrac{1}{2}\rho S C_d |\dot{x}|\dot{x} + Cx = -F_s \tag{2a}$$

$$(M_m + M_b + M_s + M_w)\ddot{x} + \tfrac{1}{2}\rho S(C_d + \Delta C_d) |\dot{x} - u|(\dot{x} - u) + D_w \dot{x} + Cx = -F_w \tag{2b}$$

In Eqs. 2a and 2b, x denotes the measured displacement of the oscillation while over dot and double over dot represent corresponding velocity and acceleration respectively. F_s and F_w are forces measured by the cantilever load cells in calm water and in waves. D_w designates the wave drift damping and ρ is the density of water. u is the orbital velocity of water particle. S represents the frontal area of the cylinder. In the case when cylinder array is used as the test model, this area should

be multiplied by the number of cylinders. C_d and ΔC_d denote the drag coefficient and the increase of the drag coefficient due to waves respectively. According to our previous experience, the contribution from the drag is about 2% of total force. Hence, terms associated with C_d and ΔC_d are neglected in the present work. Since the other motion modes are not significant according to the observation during the tests, the effects of coupling motions are not included in the present work.

Then, the Fourier analysis is applied to the recorded time histories of the displacement x and force F_s (or F_w). The low-frequency components are filled out and can be expressed as

$$x_{s,w} = A_{1s,w}\cos\sigma t + B_{1s,w}\sin\sigma t = \mathrm{Re}\left\{\left(A_{1s,w} + iB_{1s,w}\right)e^{-i\sigma t}\right\} \quad (3a)$$

$$F_{s,w} = A_{2s,w}\cos\sigma t + B_{2s,w}\sin\sigma t = \mathrm{Re}\left\{\left(A_{2s,w} + iB_{2s,w}\right)e^{-i\sigma t}\right\} \quad (3b)$$

where A_1, B_1 and A_2, B_2 are Fourier coefficients of displacement and force obtained from the Fourier analysis, respectively while σ denotes the frequency of the forced oscillation. The subscript s or w means that tests are carried out in still water or in waves respectively.

Substituting Eqs. 3a and 3b into Eqs. 2a and 2b, the added mass in calm water is obtained by

$$M_s = \frac{C}{\sigma^2} + \frac{A_{1s}A_{2s} + B_{1s}B_{2s}}{\sigma^2\left(A_{1s}^2 + B_{1s}^2\right)} - \left(M_m + M_b\right) \quad (4a)$$

On the other hand, the wave drift added mass is determined by

$$M_w = \frac{C}{\sigma^2} + \frac{A_{1w}A_{2w} + B_{1w}B_{2w}}{\sigma^2\left(A_{1w}^2 + B_{1w}^2\right)} - \left(M_m + M_b\right) - M_s \quad (4b)$$

CALCULATION METHOD

The problem considered here is that an assembly of circular cylinders is slowly oscillating in a train of regular waves. The frequency of the forced slow oscillation is designated by σ while the wave frequency is given by ω. It is assumed that σ is much smaller than ω. The depth of the calm water is equal to h. The radius of the cylinders is a and the draught is d. The cylinders are restrained from the linear responses to the incident waves. A Cartesian coordinate system following the forced slow oscillation is adopted to describe the problem. The oxy plane coincides with the undisturbed free surface while the z-axis is pointing upward. The x-axis is in the direction of the slow oscillation so that the slow oscillation is considered as a surge motion. The displacement and velocity of it are represented by $\xi(t) = \mathrm{Re}\{i\bar{\xi}e^{-i\sigma t}\}$ and $\dot{\xi}(t) = \mathrm{Re}\{\sigma\bar{\xi}e^{-i\sigma t}\}$ respectively. Here, $\bar{\xi}$ is the amplitude of the slow oscillation, which is assumed to be a real number without losing generality since the incident wave amplitude ζ_0 can be considered having a phase lag referring to the moving frame. The coordinates of oscillating frame is related to a space-fixed frame, say $OXYZ$, as follows:

$$X = x - \xi(t), \quad Y = y, \quad Z = z \quad (5)$$

The time derivative in the space-fixed frame can be transferred to the moving frame by chain-rule differentiation:

$$d/dt = \partial/\partial t - \dot{\xi}(t)\partial/\partial x \quad (6)$$

The advantage of using a moving frame is that it is not necessary to assume the amplitude of the slow oscillation to be small so that the model will be closer to the practical slow drift motion of the ocean structures.

The fluid is assumed to be inviscous and the flow to be irrotational. Therefore, there exists a velocity potential $\Phi(\boldsymbol{x}, t)$. As mentioned before, the frequency σ of the slow oscillation is much smaller compared to the incident wave frequency ω. It is natural to use two time scales to describe these two kinds of motions. Following the approach of Newman's [12], the velocity potential can be expressed by the following perturbation expansion up to the quadratic order in wave amplitude ζ_a:

$$\begin{aligned}\Phi(\boldsymbol{x},t) = \mathrm{Re}\Big\{&\phi_1(\mathbf{x})e^{-iS(t)} + \phi_2^{(0)}(\mathbf{x}) + \ldots + \sigma\bar{\xi}\left[\phi_{0\xi}(\mathbf{x})e^{-i\sigma t}\right.\\ &\left.+ \phi_{1\xi}^{(+)}(\mathbf{x})e^{-i(S(t)+\sigma t)} + \phi_{1j\xi}^{(-)}(\mathbf{x})e^{-i(S(t)-\sigma t)} + \phi_{2\xi}^{(0)}(\mathbf{x})e^{-i\sigma t} + \ldots\right]\Big\}\end{aligned} \quad (7)$$

In Eq. 7, the number in the subscript indicates the order in wave amplitude while the letter ξ denotes that the potential is related to the slow motion. Superscripts are used if necessary to indicate harmonic time dependence on the wave frequency. Here, potentials associated with double wave frequency are omitted since they will not contribute to the wave-drift added mass and damping. The phase function $S(t)$ is defined as

$$S(t) = \omega t - \xi(t)k_0\cos\beta \quad (8)$$

where k_0 is the wave number of the incident waves and β is the incident wave angle. This definition comes from the incident wave potential, which is the only specified component in the first order potential $\phi_1(\boldsymbol{x})$, expressed in the moving frame:

$$\Phi_{1I}(\mathbf{x},t) = \mathrm{Re}\left\{\phi_{1I}e^{-iS(t)}\right\} \quad (9a)$$

$$\text{with } \phi_{1I}(\mathbf{x}) = \frac{\zeta_a g}{i\omega}\frac{\cosh k_0(z+h)}{\cosh k_0 h}\exp[ik_0(x\cos\beta + y\sin\beta)] \quad (9b)$$

where g is the gravitational acceleration.

The potentials of all the orders are governed by the Laplace equation in the fluid domain and satisfy an impermeable condition on the sea bottom z=-h and the body surface S_0. On the free surface, the total velocity potential, $\Phi(\boldsymbol{x}, t)$, satisfies a nonlinear boundary condition at the exact wave elevation $z=\zeta(x, y, t)$. It is transformed to the mean free surface, z=0 by a Taylor expansion. Substituting the perturbation expansion of the velocity potential expressed in Eq. 7 into the free surface condition and resorting terms with the same order and time dependence, it yields the free surface condition for each order of potential on z=0. At the far field, i.e. a large distance from the body, a suitable radiation condition of outgoing waves is satisfied by each order of potentials except for the incident wave potential. Detail discussion on the boundary value problems and their solutions is referred to our previous work [1].

Once the potentials are solved, the hydrodynamic pressure p can be obtained by the Bernoulli equation. The wave loads are evaluated by the integration of the hydrodynamic pressure along the instantaneous wetted body surface $\tilde{S}_0$, which consists of two parts, i.e. a mean wetted body surface S_0 under the calm water and a surface wetted by the wave elevation ζ along the water line C_0 of the body.

$$\begin{aligned}F_i(t) &= \int_{\tilde{S}_0} pn_i ds\\ &= -\rho\int_{\tilde{S}_0}\left(\Phi_t - \dot{\xi}(t)\Phi_x + \tfrac{1}{2}\nabla\Phi\cdot\nabla\Phi + gz\right)n_i ds\\ &= -\rho\int_{S_0}\left(\Phi_t - \dot{\xi}(t)\Phi_x + \tfrac{1}{2}\nabla\Phi\cdot\nabla\Phi\right)n_i ds\\ &\quad + \rho/(2g)\int_{C_0}\Phi_t\left[\Phi_t - 2\dot{\xi}(t)\Phi_x + \nabla\Phi\cdot\nabla\Phi - 1/g\,\Phi_t\Phi_{tz}\right]dl\end{aligned} \quad (10)$$

where the wave elevation ζ expressed as

$$\begin{aligned}\zeta = &-1/g\left[\Phi_t - \dot{\xi}(t)\Phi_x + \tfrac{1}{2}\nabla\Phi\cdot\nabla\Phi\right.\\ &\left. - 1/g\,\Phi_t\left(\Phi_{tz} - \dot{\xi}(t)\Phi_{xz}\right) + 1/g\,\dot{\xi}(t)\Phi_x\Phi_{tz}\right]_{z=0} + O\left(\Phi^3\right)\end{aligned} \quad (11)$$

has been applied. The subscript i=1, 2, and 6 denotes the force component in surge, sway and yaw direction respectively and ρ represents the density of the fluid.

The wave forces are expanded into a perturbation series in the same way as the velocity potential with two time scales, i.e.

$$\begin{aligned}F_i(t) = \mathrm{Re}\Big\{&F_{1i}e^{-i\omega t} + F_{2i}^{(0)} + \ldots + \sigma\xi\left[F_{0i\xi}e^{-i\sigma t}\right.\\ &\left.+ F_{1i\xi}^{(+)}e^{-i(\omega+\sigma)t} + F_{1i\xi}^{(-)}e^{-i(\omega-\sigma)t} + F_{2i\xi}^{(0)}e^{-i\sigma t} + \ldots\right]\Big\}\end{aligned} \quad (12)$$

The expansion of the potential shown in Eq. 7 is then substituted into Eq. 10. By comparing with Eq. 12, forces of each order can be obtained.

We are interested in the force components with low frequency

associated with slow oscillation in the limiting case of σ being asymptotically small. In Eq. 12, $F_{0i\xi}$ is the linear force in the i-th direction per unit velocity of slow surge oscillation and is related to the linear added mass $A_{0i\xi}$ and wave-radiating damping $B_{0i\xi}$ as below:

$$F_{0i\xi} = -\left(-i\sigma A_{0i\xi} + B_{0i\xi}\right) = i\sigma\rho\int_{S_0}\phi_{0\xi}n_i ds \tag{13}$$

In the limiting case that σ tends to zero, the linear radiation potential $\phi_{0\xi}$ of the slow oscillation tends to satisfy a rigid wall condition on the free surface. The solution of it is a real function. Hence, as σ tends to zero, the linear wave-radiating damping $B_{0i\xi}$ vanishes asymptotically while the added mass tends to

$$A_{0i\xi} = \rho\int_{S_0}\phi_{0\xi}n_i ds \tag{14}$$

When i=1 in Eq. 14, $A_{01\xi}$ is equivalent to M_s in the experimental results.

On the other hand, $F_{2ij}^{(0)}$ is a force component in quadratic order of wave amplitude, which can also be separated into two parts, i.e. in phase with the acceleration and the velocity of the slow oscillation respectively.

$$F_{2i\xi}^{(0)} = -\left(-i\sigma A_{2i\xi} + B_{2i\xi}\right) \tag{15}$$

The real part of it is involved in the calculation of the wave-drift damping $B_{2i\xi}$, which is given in Newman's paper [12]. We are interested in the imaginary part of the force component $F_{2ij}^{(0)}$, i.e.

$$\begin{aligned}\sigma A_{2i\xi} = \mathrm{Im}\Big\{&-\rho\int_{S_0}\Big[-i\sigma\phi_{2\xi}^{(0)} + \nabla\phi_{0\xi}\cdot\nabla\phi_2^{(0)} + \tfrac{1}{2}\nabla(\phi_{1\xi}^{(+)} \\ &-\phi_{1\xi}^{(-)})\cdot\nabla\phi_1^*\Big]n_i ds + \frac{\rho}{2g}\int_{C_0}\Big[\omega^2\left(\phi_{1\xi}^{(+)} - \phi_{1\xi}^{(-)}\right)\phi_1^* \\ &+\sigma\omega(\phi_{1\xi}^{(+)} + \phi_{1\xi}^{(-)})\phi_1^* - \tfrac{1}{2}i\sigma\phi_{0\xi}\nabla\phi_1\cdot\nabla\phi_1^* - \tfrac{1}{2}i\omega(\phi_1\nabla\phi_1^* \\ &-\phi_1^*\nabla\phi_1)\cdot\nabla\phi_{0\xi} + i\sigma\nu(\tfrac{1}{2}\phi_{0\xi z} + \nu\phi_{0\xi})\phi_1\phi_1^*\Big]n_i dl\Big\}\end{aligned} \tag{16}$$

When σ tends to zero, we have

$$\begin{aligned}\phi_{1\xi}^{(+)} + \phi_{1\xi}^{(-)} &= \psi_0 \\ \phi_{1\xi}^{(+)} - \phi_{1\xi}^{(-)} &= \sigma\psi_1\end{aligned} \tag{17}$$

Noticing the solution of $\phi_{0\xi}$ and $\phi_2^{(0)}$ to be real, the wave-drift added mass $A_{2i\xi}$ is evaluated by

$$\begin{aligned}A_{2i\xi} = \mathrm{Im}\Big\{&-\rho\int_{S_0}\Big[-i\phi_{2\xi}^{(0)} + \nabla\psi_1\cdot\nabla\phi_1^*\Big]n_i ds \\ &+\frac{\rho}{2g}\int_{C_0}\Big[2\omega(\psi_0 + \omega\psi_1)\phi_1^* + i\nu^2\phi_{0\xi}\phi_1\phi_1^* \\ &-\tfrac{i}{2}\phi_{0\xi}\nabla\phi_1\cdot\nabla\phi_1^*\Big]n_i dl\Big\}\end{aligned} \tag{18}$$

in the limiting case of asymptotically small σ. When i=1 in Eq. 18, $A_{21\xi}$ is equivalent to M_w in the experimental results.

It can be observed that the higher order potentials ψ_1 and $\phi_{2\xi}^{(0)}$ make contribution to the wave-drift added mass. This contribution is not included in the present work since these two potentials remain unsolved.

RESULTS AND COMPARISON

Experimental results are presented and compared with calculated results in this section.

First, the effects of the wave amplitude are examined. The ratio of wave drift added mass to the added mass in still waver, i.e. M_w/M_s, is plotted against nondimensional wave amplitude ζ_a/a in Fig 3 for the cylinder array. The frequency σ of the forced oscillation is 0.929 rad/sec corresponding to the draft d=2a or 1.162 rad/sec for draft d=a respectively. The normalized wave number k_0L= 5.0 in Fig 3a and k_0L= 6.0 in Fig 3b. In these figures, parabolic curves (dashed or dotted lines) of $b(\zeta_a/a)^2$ have been drawn to the corresponding experimental data. The coefficient b is determined by the least square method. It is observed that the ratio is generally proportional to the square of the wave amplitude. This confirms that the wave drift added mass is a quadratic quantity of the wave amplitude since the added mass in calm water is only linearly related to the forced oscillations and not relevant to the incident waves.

Next, the effects of the wave number are considered. The wave drift added mass M_w normalized by $N\rho\pi a\zeta_a^2$ is plotted against wave number k_0 in Fig 4. Here N is the total number of cylinders. The wave number is nondimensionalized by the radius of cylinder for the case of single cylinder (Fig 4a) while normalized by the longitudinal distance L between cylinders for the cylinder array (Fig 4b). In the case of single cylinder, the draft of the cylinder d is 3a and the frequency of the forced oscillation σ is 0.641 or 0.804 rad/sec. In the case of cylinder array, σ =0.929 rad/sec when d =2a and σ=1.137 rad/sec when d =a. Results of FD tests are also presented in this figure. The agreement between FD and FO tests is good. Calculated results, represented by lines, are presented in these figures to compare with experimental ones. It can be seen that they agree fairly well with each other in general tendency especially in the case of cylinder array although departure between these two results can also be observed. Since the linear response of the models to the incident waves and the contribution of higher order potentials are not included in the calculation as mentioned in the previous section, the difference between these two results is expectable.

Last, the effects caused by the frequency of the forced oscillation are considered. Shown in Fig. 5 is the wave drift added mass of the cylinder array, normalized in the same way as above, against the nondimensional frequency $\sigma\sqrt{L/g}$ of the forced oscillation. The draft of the cylinders is a. The wave amplitude ζ_a=0.02 or 0.03 meters while the normalized wave number k_0L=5.0. It can be observed that the wave drift added mass decreases with the increase of the forced oscillation frequency. Hence, the wave drift added mass is not a constant value at any frequency of slow oscillation. It is a complicated phenomenon relating to slow oscillation and incident waves. Further study is necessary to make a full understand of it.

CONCLUDING REMARKS

Systematic experiments are performed to measure the wave drift added mass and results are presented in the present work. The experiments consist of FD tests and FO tests. The results of these two kinds of tests agree well with each other. It can be observed that the wave drift added mass is proportional to the square of the wave amplitude, which indicates that it is a quadratic quantity of the wave amplitude. The value of the wave drift added mass is not simply a constant when the frequency of the slow oscillation is changed. This implies that it is a complicated phenomenon involving the interaction of slow oscillations and the wave motions. More effort is needed to make a full understand of it. Comparison with the calculated results shows that the calculation method should be further developed to include the effects of the linear response of the body to the incident waves and higher order potentials in terms of slow frequency.

REFERENCE

1. Bao W., Kinoshita T. (2001) "Wave-drift added mass of a cylinder array slowly oscillating in waves", *Proc. of OMAE* 2001 Rio de Nero.
2. Emmerhoff O. J., Sclavounos P. D. (1992) "The slow-drift motion of arrays of vertical cylinders". *J. Fluid Mech.* Vol. 242: 31-50
3. Finne, S., Grue J. (1998) "On the complete radiation-diffraction problem and wave-drift damping of marine bodies in the yaw mode of motion". *J. Fluid Mech.* Vol. 357: 289-320.
4. Grue J., Palm E. (1993) "The mean drift force and yaw moment on marine structures in waves and current". *J. Fluid Mech.* Vol. 250: 121-145

5. Grue J., Palm E (1996) “Wave drift damping of floating bodies in slow yaw motion”. *J. Fluid Mech.* Vol. 319: 323-352.
6. Huijsmans, R. H. M., Hermans, A. J. (1985) “A fast algorithm for computation of 3-D ship motions at moderate forward speed”. *4th Intl Conf. on Numerical Ship Hydrodynamics* (ed. J. H. MaCarthy). National Academy of Science Press, Washington.
7. Huijsmans, R. H. M. (1986) “Wave drift forces in current”. *16th Symp. on Naval Hydrodynamics.* Berkeley. National Academy of Science Press, Washington.
8. Kinoshita T., Takaiwa K. (1990) “Added mass increase due to waves for slow drift oscillation of a moored semi-submersible”, *Proc. of OMAE* 1990, Houston.
9. Kinoshita T., Shoji K., Obama H. (1992) “Low frequency added mass of a semi-submersible influenced by incident waves”, *Proc. of ISOPE* 1992, San Francisco.
10. Kinoshita, T., Bao, W. (1996) “Hydrodynamic forces acting on a circular cylinder oscillating in waves and a small current”. *J. Marine Sci Technol,* Vol. 1:155-173
11. Matsui T, Lee S. Y., Sano K (1991) “Hydrodynamic forces on a vertical cylinder in current and Waves” (in Japanese) *J Soc of Naval Archit of Japan,* Vol. 170: 277-287.
12. Newman J.N. (1993) “Wave-drift damping of floating bodies”. *J. Fluid Mech.* Vol.249; 241-259.
13. Nossen, J., Grue, J., Palm, E. (1991) “Wave forces on three-dimensional floating bodies with small forward speed”. *J. Fluid Mech.* Vol. 227, 135-160.
14. Wichers, J.E.W., Sluijs, M. F. van (1979) “The influence of waves on the low frequency hydrodynamic coefficients of moored vessels”, *Proc. of Offshore Technology Conf.*, Houston, OTC 3625.
15. Zhao, R, Faltinsen, O. M. (1989) “Interaction between current, waves and marine structures”. *5th Intl Conf. on Numerical Ship Hydrodynamics, Hiroshima* (ed. K. Mori), National Academy of Science Press, Washington.

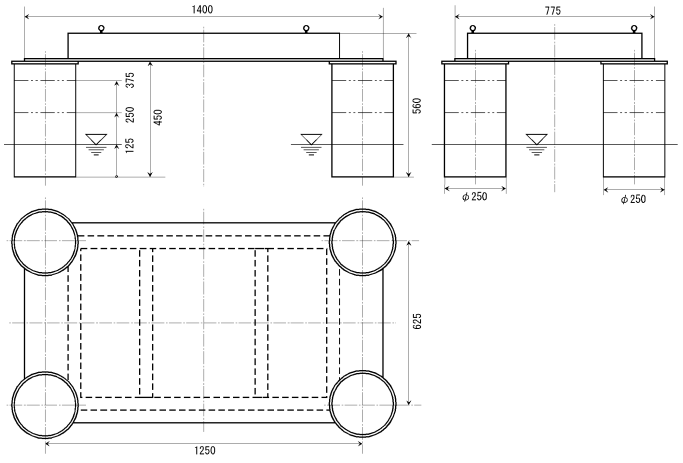

Fig 1. Schematic figures of a cylinder array used in the experiment.

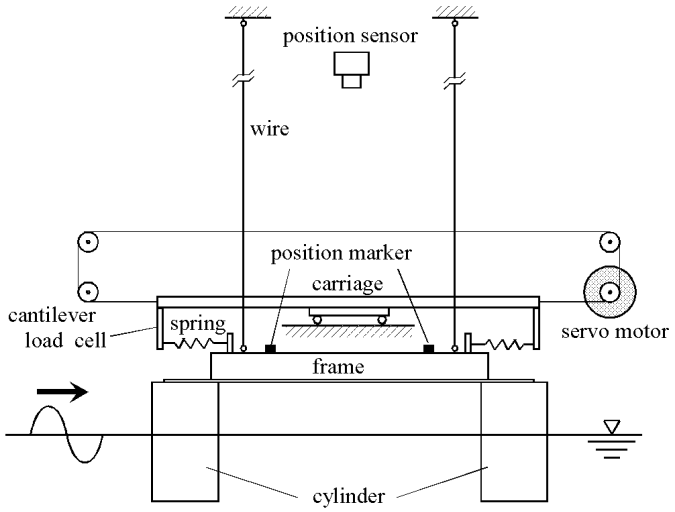

Fig 2. Setting-up of the experiment equipments.

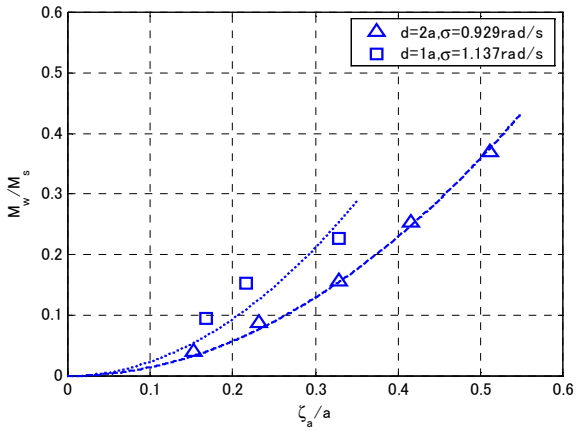

(a)

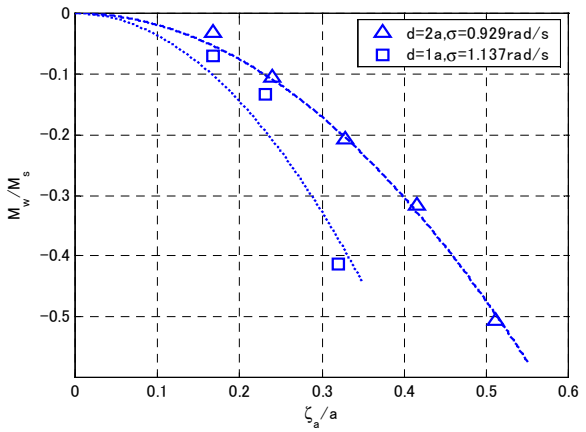

(b)

Fig 3. The effects of wave amplitude on the wave drift added mass of the cylinder array. (a) k_0L= 5.0; (b) k_0L= 6.0.

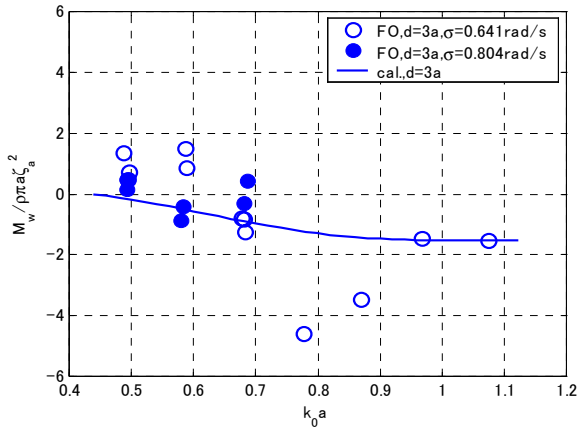

(a)

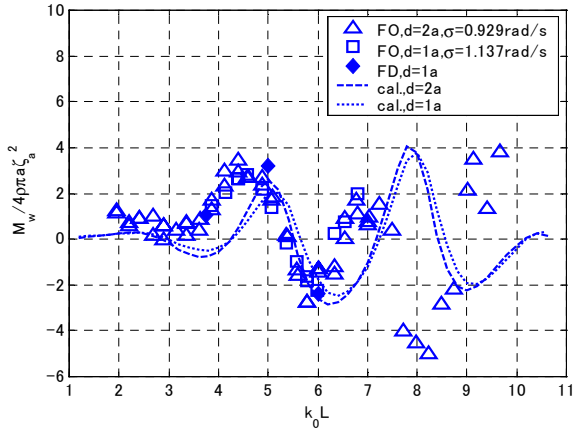

(b)

Fig 4. Effects of wave number on the wave drift added mass. (a) Results of a single cylinder; (b) results of the cylinder array.

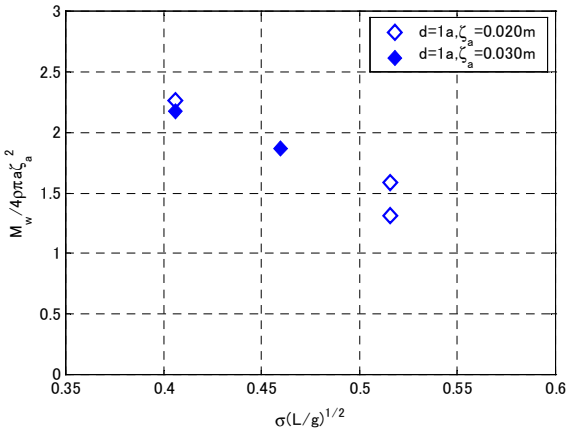

Fig 5. Effects of slow oscillation frequency on the wave drift added mass of the cylinder array.